

*A quasistatic mixed-mode delamination model*

*Tomáš Roubíček, Vladislav Mantič, Christos G. Panagiotopoulos*

Preprint no. 2011-020



Research Team 1  
Mathematical Institute of the Charles University  
Sokolovská 83, 186 75 Praha 8  
<http://ncmm.karlin.mff.cuni.cz/>

---

This is a preprint version of the paper to be published in AIMS' journal "Discrete and Cont. Dynam. Syst.". The preprint and its maintaining in this preprint series is in accord with the AIMS' copyright agreement, in particular it is 'for the purposes of research for a non commercial purpose or for private study' only.

---

# A quasistatic mixed-mode delamination model<sup>1</sup>

TOMÁŠ ROUBÍČEK<sup>1,2</sup>, V. MANTIČ,<sup>3</sup> C.G. PANAGIOTOPOULOS<sup>3</sup>

<sup>1</sup> Mathematical Institute, Charles University, Sokolovská 83, CZ-186 75 Praha 8, Czech Republic,

<sup>2</sup> Institute of Thermomechanics of the ASCR, Dolejškova 5, CZ-182 00 Praha 8, Czech Republic.

<sup>3</sup> Group of Elasticity and Strength of Materials, Dept. of Continuum Mech., School of Engineering, University of Seville, Camino de los Descubrimientos s/n, ES-41092 Sevilla, Spain.

**Abstract.** The quasistatic rate-independent evolution of a delamination in the so-called mixed mode, i.e. distinguishing opening (Mode I) from shearing (Mode II), devised in [45], is rigorously analysed as far as existence of the so-called energetic solutions concerns. The model formulated at small strains uses a delamination parameter of Frémond’s type combined with a concept of an interface plasticity, and is associative in the sense that the dissipative force driving the delamination has a potential which depends in a 1-homogeneous way only on rates of internal parameters. A sample numerical simulation documents that this model can really produce mixity-sensitive delamination.

*AMS Classification:* 35K85; Secondary: 49S05, 74R20.

*Keywords:* Rate-independent interface fracture, inelastic debonding, variational inequality, energetic solution, Rothe method, convergence analysis, simulations.

**1. Introduction, rate-independent processes, delamination.** A basic model for quasistatic delamination (sometimes also called debonding), proposed by Frémond [13, 14], involves a damage-type variable called *delamination parameter* and denoted by  $\zeta$ . It reflects the destruction of the bonds in the a-priori given delamination surfaces or part of outer boundary  $\Gamma_C$ . Here  $\zeta=0$  means that no effective adhesion exists while for  $\zeta=1$  the microscopic bonds between the bodies are fully effective. This basic model incorporates merely the *Griffith concept* [18], namely the philosophy that the crack grows as soon as the so-called energy release rate is bigger than the phenomenologically prescribed fracture-activation energy (per unit area of a new crack surface), called also *fracture toughness*. This activation energy is simultaneously equal to the dissipated energy if delamination is completed. As such, the energy needed (and dissipated) for delamination is rate-independent, which (after neglecting all inertial/viscous/thermal effects) leads to the *rate-independent* quasistatic model. The weak surface undergoing delamination can be considered either purely brittle or brittle-elastic, the latter case reflecting that the adhesive gluing this weak surface has a certain elastic response. This approach was developed in [23, 41–43, 46], cf. also [15, Chap.14]. Alternatively, there are models that, instead of a delamination parameter defined on the delaminating surface, a-priori prescribe the geometry of the delaminated part (usually in 2-dimensional situation just as one segment on a 1-dimensional surface), cf. [22, 37, 54]. We will focus on the first type of models.

Engineering models of delamination are, however, more complicated than the mere Griffith model: the dissipated energy in the so-called mode I (delamination by opening) is less than in the so-called mode II (delamination by plane shearing); sometimes, the difference may be tens or even hundred percents and, in general loading, it depends on the so-called *fracture-mode mixity* [2, 24, 25, 48]. Microscopically, the additional dissipation in mode II may be explained by a certain plastic processes both in the adhesive itself and in a narrow bulk vicinity of the delamination surface before the actual delamination starts [24, 56], or by some rough structure of the interface [12]. In a certain idealization, these plastic processes are more relevant in mode II while do not manifest significantly in mode I if the plastic strain is considered in  $\mathbb{R}_{\text{dev}}^{d \times d}$  which is the linear space of

---

<sup>1</sup>The authors are very thankful to Professor Roman Vodička for careful critical reading of the manuscript leading to a lot of improvements. Moreover, V.M. and C.G.P. acknowledge the support by the Junta de Andalucía (Proyecto de Excelencia TEP-4051). C.G.P. also acknowledges the hospitality of Charles University, where this work has partly been accomplished, supported by the “Nečas center for mathematical modeling” LC 06052 (MŠMT ČR). T.R. acknowledges the hospitality of Universidad de Sevilla, where this work has partly been accomplished, covered by Junta de Andalucía through the project IAC 09-III-6321, as well as partial support from the grants A 100750802 (GA AV ČR), 201/09/0917 and 201/10/0357 (GA ČR), and MSM 21620839 (MŠMT ČR), and from the research plan AV0Z20760514 (ČR)

‘incompressible’ (=trace free) symmetric strains. Modelling a narrow plastic stripe around  $\Gamma_C$  is computationally difficult, and thus simplified phenomenological models are worth considering.

An immediate reflection of the above phenomenon adopted in the standard engineering approach, as e.g. in [4, 20, 49, 50], is making the activation energy dependent on the so-called fracture-mode-mixity angle, i.e. on the ratio of normal/tangential component of displacement jump or traction vector. This state-dependence of the dissipation rate makes such models non-associative (meaning that no specific activation threshold can be associated to the flow-rule governing the inelastic delamination process). The mathematical analysis of such models is, in general, difficult and, in particular, is missing for such quasistatic models of delamination. Only recently an analysis has been made for an augmented model using Kelvin-Voigt rheology and nonsimple material concept [44]. This is an ultimate motivation to devise an *associative model* (governed by a dissipation potential independent of the state and thus fully determined by an associated activation threshold, cf.  $K$  in (6) below) which would be amenable to mathematical analysis but still exhibiting a fracture-mode-mixity sensitivity. Such a model, presented in detail in Section 2, has essentially been devised in [45, Sect.5.2] however without any rigorous mathematical analysis and experimental justification.

The goal of this article is to analyse from the theoretical viewpoint some basic features of this associative model including a plastic-type variable  $\pi$  defined on  $\Gamma_C$  in addition to the delamination variable  $\zeta$ . In particular, in Section 3, we will show the existence of the so-called energetic solutions (cf. Definition 1 below). Moreover, in Section 4, we will validate this model by a sample 2-dimensional simulation, showing that it can really produce expected responses.

**2. Associative model.** We will consider the evolution on a fixed finite time interval  $[0, T]$  governed by a *stored energy* functional  $\mathcal{E} : [0, T] \times \mathcal{U} \times \mathcal{Z} \rightarrow \mathbb{R} \cup \{\infty\}$  and a *dissipated energy* functional  $\mathcal{R} : \mathcal{X} \rightarrow [0, \infty]$ , where  $\mathcal{U}$  stands for the linear space of displacements fields  $u$ ,  $\mathcal{Z}$  for that of “inelastic” parameters fields  $z = (\zeta, \pi)$  (i.e. here delamination and interface-plasticity parameters) while  $\mathcal{X}$  for time derivatives of  $z$ . Specification of these energy functionals will be given later on. The rate-independent evolution we have in mind is governed by the following system of *doubly nonlinear* degenerate abstract *static/evolution inclusions*, referred sometimes as Biot’s equations generalizing the original work [5, 6]:

$$\partial_u \mathcal{E}(t, u, z) \ni 0 \quad \text{and} \quad \partial \mathcal{R}(\dot{z}) + \partial_z \mathcal{E}(t, u, z) \ni 0, \quad (1)$$

where  $\dot{z} := \frac{dz}{dt}$  and the symbol “ $\partial$ ” refers to a (partial) subdifferential, relying on that  $\mathcal{R}(\cdot)$ ,  $\mathcal{E}(t, \cdot, z)$ , and  $\mathcal{E}(t, u, \cdot)$  are convex functionals.

Classical models for Griffith-type delamination only consider interface delamination processes described by a single internal delamination variable  $\zeta$  defined on the interface  $\Gamma_C$ . However, the philosophy of the present associative model is to take into account an additional inelastic process on  $\Gamma_C$ , which would be activated rather in fracture mode II than in mode I, and thus more energy would be dissipated in mode II than in mode I. This inelastic process involves an additional dissipative variable  $\pi$  having the meaning of the plastic-like *tangential slip* on  $\Gamma_C$ .

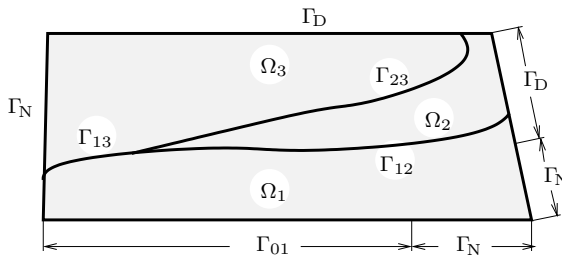


Fig. 1. Schematic illustration of the geometry and of the notation for 2-dimensional case of 3 mutually bonded subdomains, i.e.  $d=2$  and  $N=3$ .

To formulate the model, we consider  $\Omega \subset \mathbb{R}^d$  ( $d = 2, 3$ ) a bounded Lipschitz domain, and its decomposition into a finite number of mutually disjoint Lipschitz subdomains  $\Omega_i$ ,  $i = 1, \dots, N$ ,

see Fig. 1. We denote formally  $\Omega_0 := \mathbb{R}^d \setminus \bar{\Omega}$ . Further we denote with  $\Gamma_{ij} = \partial\Omega_i \cap \partial\Omega_j$  the (possibly empty) boundary between  $\Omega_i$  and  $\Omega_j$ ,  $i, j = 1, \dots, N$ .  $\Gamma_{ij}$  represents a prescribed  $(d-1)$ -dimensional surface, which may undergo delamination. We also consider possible delamination on some parts of the outer boundary  $\Gamma_{0i} \subset (\partial\Omega \cap \bar{\Omega}_i)$ , cf. Fig. 3 below. The union of these parts is denoted as  $\Gamma_0 = \bigcup_{1 \leq i \leq N} \Gamma_{0i}$ . We assume that the rest of the outer boundary  $\partial\Omega$ , i.e.  $\partial\Omega \setminus \Gamma_0$ , is the union of two disjoint subsets  $\Gamma_D$  and  $\Gamma_N$ , with

$$\mathcal{L}^{d-1}(\partial\Omega_i \cap \Gamma_D) > 0, \quad i = 1, \dots, N, \quad (2)$$

where  $\mathcal{L}^{d-1}$  denotes the  $(d-1)$ -dimensional Lebesgue measure. On the Dirichlet part of the boundary  $\Gamma_D$  and on  $\Gamma_0$  we impose a time-dependent boundary displacement  $w_D(t)$ , while the boundary  $\Gamma_N$  is considered free. This means that, any admissible displacement  $u : \bigcup_{i=1}^N \Omega_i \rightarrow \mathbb{R}^d$  has to be equal to  $w_D(t)$  on  $\Gamma_D$  (defining a kind of ‘‘hard-device’’ loading) and has to satisfy  $(w_D(t) - u) \cdot \nu \geq 0$  on  $\Gamma_0$ , where  $\nu$  is the unit outward normal of  $\partial\Omega$ . Thus, inelastic delamination can be developed on the surface

$$\Gamma_C := \bigcup_{0 \leq i < j \leq N} \Gamma_{ij}. \quad (3)$$

For readers convenience, let us summarize the basic notation used in what follows:

$u$ displacements	$\kappa_t$ distributed tangential stiffness
$\zeta$ damage scalar variable	$\kappa_H$ plastic modulus of kinematic hardening
$\pi$ interfacial plastic slip	$\kappa_0$ delamination gradient coefficient
$e(u)$ small strain tensor	$\sigma_{t,\text{yield}}$ yield shear stress
$\mathbb{C}$ elastic-moduli tensor	$a_I$ energy released per unit area in pure mode I
$\kappa_n$ distributed normal stiffness	$a_{II}$ energy released per unit area in pure mode II

First we present in detail a plastic-type model with kinematic-type hardening (like e.g. in [19,47]) for the above described delamination problem, devised essentially in [45] without any mathematical/computational justification, however. This model is described by the stored-energy functional

$$\mathcal{E}(t, u, \zeta, \pi) := \begin{cases} \sum_{i=1}^N \int_{\Omega_i} \frac{1}{2} \mathbb{C}^{(i)} e(u) : e(u) \, dx \\ \quad + \int_{\Gamma_C} \left( \zeta \left( \frac{\kappa_n}{2} |[[u]]_n|^2 + \frac{\kappa_t}{2} |[[u]]_t - \pi|^2 \right) \right. \\ \quad \left. + \frac{\kappa_H}{2} |\pi|^2 + \frac{\kappa_0}{r} |\nabla_S \zeta|^r \right) \, dS & \text{if } u = w_D(t) \text{ on } \Gamma_D, \\ & 0 \leq \zeta \leq 1 \text{ on } \Gamma_C, \\ & [[u]]_n \geq 0 \text{ on } \Gamma_C, \\ \infty & \text{elsewhere,} \end{cases} \quad (4a)$$

with  $r > d-1$  and  $\kappa_0 > 0$ , and by the dissipation-energy potential

$$\mathcal{R}(\dot{z}) = \mathcal{R}(\dot{\zeta}, \dot{\pi}) := \begin{cases} \int_{\Gamma_C} a_I |\dot{\zeta}| + \sigma_{t,\text{yield}} |\dot{\pi}| \, dS & \text{if } \dot{\zeta} \leq 0 \text{ a.e. on } \Gamma_C, \\ \infty & \text{otherwise,} \end{cases} \quad (4b)$$

with  $\mathbb{C}^{(i)}$  being the elastic-moduli tensor at the particular subdomain  $\Omega_i$  and  $e(u) = \frac{1}{2}(\nabla u)^\top + \frac{1}{2}\nabla u$  denotes the small strain tensor,  $\nabla_S$  a ‘‘surface gradient’’ (i.e. the tangential derivative defined as  $\nabla_S v = \nabla v - (\nabla v \cdot \nu)\nu$  for  $v$  defined on  $\Gamma_C$ ), and  $[[u]] = [[u]]_n \nu + [[u]]_t$  with  $[[u]]_n = [[u]] \cdot \nu$ ,  $\nu$  being a unit normal to  $\Gamma_C$ . In fact, the model naturally does not depend on the chosen orientation, although for  $\Gamma_0$  the outward normal  $\nu$  is typically taken. Here we used the notation  $[[u]]$  as the differences of traces from both sides of  $\Gamma_C$ . On  $\Gamma_0$ , we also used the convention that  $w_D$  stands for the prescribed trace from  $\Omega_0 := \mathbb{R}^d \setminus \bar{\Omega}$ , defining  $[[u]] = w_D(t) - u$  therein. The phenomenological elastic constants  $\kappa_n$  and  $\kappa_t$  in (4a) describe the stiffnesses of the linearly elastically responding adhesive in the normal and tangential directions, respectively. Typical phenomenology is that  $\kappa_n$

is greater than  $\kappa_t$ . In particular, for an isotropic adhesive in plane strain, the condition  $\kappa_n/\kappa_t \geq 2$  has been deduced in [50] (see also further references therein).

The dissipation potential  $\mathcal{R}$  from (4b) has a local character and can be written as

$$\mathcal{R}(\dot{z}) = \mathcal{R}(\dot{\zeta}, \dot{\pi}) := \int_{\Gamma_C} \delta_K^*(\dot{\zeta}, \dot{\pi}) \, dS \quad (5)$$

for a suitable non-negative, convex, degree-1 homogeneous function  $\delta_K^* : \mathbb{R}^d \rightarrow [0, \infty]$ ; this function is called a gauge and we have used that it can always be written as the Legendre-Fenchel conjugate  $(\cdot)^*$  to the indicator function  $\delta_K$  of a certain convex closed set  $K \ni 0$ . The boundary of this set  $K$  plays the role of a yield stress, i.e. activation stress for triggering the inelastic evolution of  $(\zeta, \pi)$ . In the specific case (4b), we have

$$K = [-a_1, \infty) \times \{|\cdot| \leq \sigma_{t,\text{yield}}\}. \quad (6)$$

Indeed, it is easy to verify that, for  $K$  from (6), it holds

$$\begin{aligned} \delta_K^*(\dot{\zeta}, \dot{\pi}) &:= \sup_{\xi, \eta} \dot{\zeta}\xi + \dot{\pi}:\eta - \delta_K(\xi, \eta) = \sup_{\xi \geq -a_1, |\eta| \leq \sigma_{t,\text{yield}}} \dot{\zeta}\xi + \dot{\pi}:\eta \\ &= \sup_{|\eta| \leq \sigma_{t,\text{yield}}} \dot{\pi}:\eta + \sup_{\xi \geq -a_1} \dot{\zeta}\xi = \sigma_{t,\text{yield}}|\dot{\pi}| + \begin{cases} a_1|\dot{\zeta}| & \text{if } \dot{\zeta} \leq 0, \\ \infty & \text{elsewhere,} \end{cases} \end{aligned} \quad (7)$$

which is just (4b)–(5).

To facilitate the construction of a mutual recovery sequence, cf. (30) below, we have used a gradient theory for internal parameters; for such concepts see, e.g. [1, 3, 7, 8, 15, 16, 21] and in the context of delamination in particular [15, Chap.14] or [7, 8]. In fact, it suffices to use gradients only of  $\zeta$  or of  $\pi$ . In (4a), we have chosen the first option, namely a gradient theory for  $\zeta$ . For the other option, see Remark 3 below. In case  $d = 3$ , the physical dimensions are:  $[a_1] = [a_{\text{II}}] = \text{J}/\text{m}^2$ ,  $[\sigma_{t,\text{yield}}] = \text{J}/\text{m}^3 = \text{N}/\text{m}^2$ , and  $[\kappa_t] = [\kappa_n] = [\kappa_{\text{H}}] = \text{J}/\text{m}^4 = \text{N}/\text{m}^3$ , while  $[\xi] = \text{J}/\text{m}^2$  and  $[\eta] = \text{J}/\text{m}^3$ . Assuming  $\kappa_0 = 0$ , the activation criterion to trigger delamination is now

$$\frac{1}{2} \left( \kappa_n |\llbracket u \rrbracket_n|^2 + \kappa_t |\llbracket u \rrbracket_t - \pi|^2 \right) \leq a_1. \quad (8)$$

Starting from the initial conditions

$$\pi(0, \cdot) = \pi_0 = 0 \quad \text{and} \quad \zeta(0, \cdot) = \zeta_0 = 1, \quad (9)$$

the response in pure mode I is essentially determined by  $\kappa_n$  and  $a_1$  because pure opening neither triggers the evolution of  $\pi$  nor causes  $\llbracket u \rrbracket_t \neq 0$ , cf. Fig. 2(left).

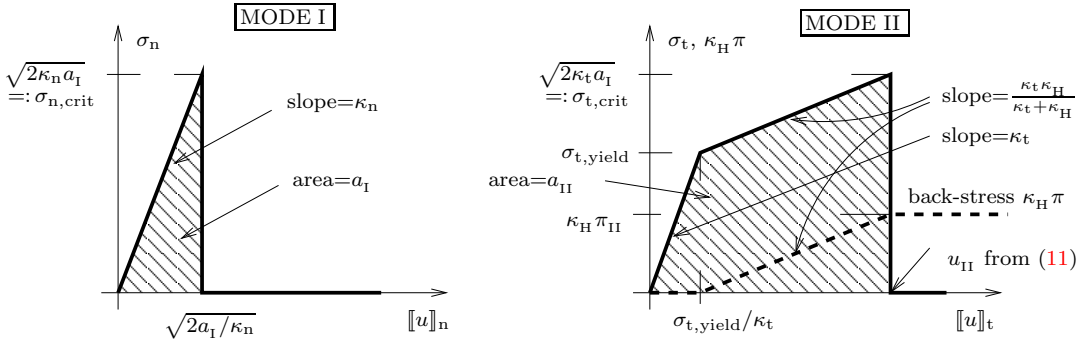


Fig. 2. Schematic illustration of the stress-relative displacement law in the model (4) for  $d = 2$  under the pulling and the shearing experiments, considering  $\zeta_0 = 1$  and  $\pi_0 = 0$ . If  $2\kappa_t a_1 \geq \sigma_{t,\text{yield}}^2$ , always  $a_{\text{II}} \geq a_1$ , where  $a_{\text{II}}$  is defined by (11c). Contribution of the delamination-gradient term is neglected, i.e.  $\kappa_0 = 0$ .

To analyse the response in pure mode II, let us realize that the tangential stress  $\sigma_t$  is a derivative of  $\mathcal{E}$  with respect to  $\llbracket u \rrbracket_t$ , and thus  $\sigma_t = \sigma_t(u, \pi) = \kappa_t(\llbracket u \rrbracket_t - \pi)$  if  $\zeta = 1$ . In analogy with the conventional plasticity, the slope of the evolution of  $\pi$  under hardening is  $\kappa_t/(\kappa_t + \kappa_{\text{H}})$ . Indeed, the evolution of  $\pi$  is governed by the flow rule

$$\dot{\pi} \in N_{\{|\cdot| \leq \sigma_{t,\text{yield}}\}}(\sigma_t - \kappa_{\text{H}}\pi) \quad \text{with} \quad \sigma_t = \zeta \kappa_t(\llbracket u \rrbracket_t - \pi) \quad (10)$$

where  $N_{\{|\cdot| \leq \sigma_{t,\text{yield}}\}}(\sigma)$  denotes the normal cone to the ball of the radius  $\sigma_{t,\text{yield}}$  at a point  $\sigma$ . Note that, the driving force  $\sigma_t - \kappa_{\text{H}}\pi$  in (10) is in a position of a negative derivative of  $\mathcal{E}$  with respect to  $\pi$ , and  $\kappa_{\text{H}}\pi$  is a so-called *back-stress* with respect to the elastic stress  $\sigma_t$ . The evolution of  $\pi$  is triggered when  $|\sigma_t - \kappa_{\text{H}}\pi|$  reaches the activation threshold  $\sigma_{t,\text{yield}}$ , and then  $|\zeta\kappa_t([\![u]\!]_t - \pi) - \kappa_{\text{H}}\pi| = \sigma_{t,\text{yield}}$ . After some algebra, we can see that  $\pi = (\zeta\kappa_t([\![u]\!]_t - \sigma_{t,\text{yield}}))/(\zeta\kappa_t + \kappa_{\text{H}})$  during evolution of  $\pi$ , which gives the mentioned slope  $\kappa_t/(\kappa_t + \kappa_{\text{H}})$  before delamination starts (i.e. when  $\zeta = 1$ ). The slope of the evolution of the back-stress  $\kappa_{\text{H}}\pi$  is then  $\kappa_t\kappa_{\text{H}}/(\kappa_t + \kappa_{\text{H}})$ , as depicted in Fig. 2(right).

From (8), one can see that delamination in pure mode II is triggered if  $\frac{1}{2}\kappa_t|[\![u]\!]_t - \pi|^2 = \frac{1}{2}\sigma_t^2/\kappa_t$  attains the threshold  $a_1$ , i.e. if the tangential stress  $\sigma_t$  achieves the critical stress  $\sigma_{t,\text{crit}} = \sqrt{2\kappa_t a_1}$ , as depicted in Fig. 2(right). Delamination in mode II is thus triggered by the tangential displacement  $u_{\text{II}}$  and the tangential slip  $\pi_{\text{II}}$  given by

$$u_{\text{II}} = \frac{\sqrt{2\kappa_t a_1}(\kappa_t + \kappa_{\text{H}}) - \sigma_{t,\text{yield}}\kappa_t}{\kappa_t\kappa_{\text{H}}}, \quad (11a)$$

$$\pi_{\text{II}} = \frac{\sqrt{2\kappa_t a_1} - \sigma_{t,\text{yield}}}{\kappa_{\text{H}}} \quad (11b)$$

and, after some algebra, one can see that the overall dissipated energy is

$$a_{\text{II}} = a_1 + \sigma_{t,\text{yield}}\pi_{\text{II}} = a_1 + \frac{\sigma_{t,\text{yield}}\sqrt{2\kappa_t a_1} - \sigma_{t,\text{yield}}^2}{\kappa_{\text{H}}} \quad (11c)$$

provided  $2\kappa_t a_1 \geq \sigma_{t,\text{yield}}^2$ , and taking into account that the evolution of  $\pi$  will stop after delamination is completed. From (11) results, after some algebra,

$$\kappa_{\text{H}}\pi_{\text{II}} = \frac{\kappa_t\kappa_{\text{H}}}{\kappa_t + \kappa_{\text{H}}}\left(u_{\text{II}} - \frac{\sigma_{t,\text{yield}}}{\kappa_t}\right), \quad (12)$$

cf. Fig. 2(right). A measure of maximum *fracture-mode sensitivity*  $a_{\text{II}}/a_1$  is then indeed bigger than 1, namely

$$\frac{a_{\text{II}}}{a_1} = 1 + \frac{\sigma_{t,\text{yield}}\pi_{\text{II}}}{a_1} = 1 + \frac{\sigma_{t,\text{yield}}}{\kappa_{\text{H}}}\sqrt{\frac{2\kappa_t}{a_1}} - \frac{\sigma_{t,\text{yield}}^2}{\kappa_{\text{H}}a_1}. \quad (13)$$

The interface plastic slip stops evolving after delamination, as depicted by the dashed line in Fig. 2(right), only if, after the delamination, the driving stress  $-\kappa_{\text{H}}\pi_{\text{II}}$  has the magnitude less than  $\sigma_{t,\text{yield}}$  (as also used for (11c)), which, in view of (11b), needs  $\kappa_t a_1 < 2\sigma_{t,\text{yield}}^2$ . Thus, to produce desired effects, our model should work with parameters satisfying

$$\frac{1}{2}\kappa_t a_1 < \sigma_{t,\text{yield}}^2 \leq 2\kappa_t a_1. \quad (14)$$

Analysing the system of abstract inclusions (1) with the specific choice of  $\mathcal{E}$  and  $\mathcal{R}$  from (4) and using the Green formulas, one can obtain a classical formulation of the problem in terms of *parabolic/elliptic variational inequalities*. After some manipulation, assuming all the interfaces and the solution sufficiently smooth, one can get the force equilibrium in each bulk domain

$$\operatorname{div}(\mathbb{C}^{(i)}e(u)) = 0 \quad \text{on } \Omega_i, \quad i = 1, \dots, N, \quad (15a)$$

as well as the equilibrium of tractions on the (interface) contact surface

$$[\![\mathbb{C}e(u)\nu]\!] = 0 \quad \text{on } \Gamma_C \setminus \Gamma_0, \quad (15b)$$

where  $[\![\mathbb{C}e(u)\nu]\!]$  denotes the difference of the tractions  $\mathbb{C}^{(i)}e(u)\nu$  and  $\mathbb{C}^{(j)}e(u)\nu$  on  $\Gamma_{ij}$ . Additionally, on the contact surface  $\Gamma_C$ , see (3), there is a condition for the tangential component of the displacement in terms of an adhesive, Robin-type condition

$$\left[ \mathbb{C}e(u)\nu - \zeta\kappa_n [\![u]\!]_n \nu - \zeta\kappa_t ([\![u]\!]_t - \pi) \right]_t = 0 \quad \text{on } \Gamma_C, \quad (15c)$$

and a unilateral Signorini adhesive contact condition in the form of the complementarity problem for the normal components

$$\llbracket u \rrbracket_n \geq 0 \quad \text{on } \Gamma_C, \quad (15d)$$

$$\left[ \mathbb{C}e(u)\nu - \zeta\kappa_n \llbracket u \rrbracket_n \nu - \zeta\kappa_t (\llbracket u \rrbracket_t - \pi) \right]_n \leq 0 \quad \text{on } \Gamma_C, \quad (15e)$$

$$\llbracket u \rrbracket_n \left[ \mathbb{C}e(u)\nu - \zeta\kappa_n \llbracket u \rrbracket_n \nu - \zeta\kappa_t (\llbracket u \rrbracket_t - \pi) \right]_n = 0 \quad \text{on } \Gamma_C. \quad (15f)$$

Note that, for non-active contact, i.e. for  $\llbracket u \rrbracket_n > 0$ , (15c,f) imply the Robin-type condition:  $\mathbb{C}e(u)\nu = \zeta\kappa_n \llbracket u \rrbracket_n \nu + \zeta\kappa_t (\llbracket u \rrbracket_t - \pi)$ . Furthermore, on the contact surface  $\Gamma_C$ , we have the flow rule for  $\zeta$  in the form of the complementarity problem

$$\dot{\zeta} \leq 0, \quad \mathfrak{s} \leq a_t, \quad \dot{\zeta}(\mathfrak{s} - a_t) = 0, \quad (15g)$$

where  $\mathfrak{s}$  denotes the driving force (here rather ‘‘driving energy’’) for  $\zeta$  defined as

$$\begin{aligned} \mathfrak{s} &= \frac{1}{2} \left( \kappa_n |\llbracket u \rrbracket_n|^2 + \kappa_t |\llbracket u \rrbracket_t - \pi|^2 \right) \\ &\quad - \operatorname{div}_S (\kappa_0 |\nabla_S \zeta|^{r-2} \nabla_S \zeta) + (\operatorname{div}_S \nu) (\kappa_0 |\nabla_S \zeta|^{r-2} \nu) + \xi \\ &\quad \text{with } \xi \in N_{[0,1]}(\zeta), \end{aligned} \quad (15h)$$

up to  $\nabla_S \zeta$ -terms, cf. also (8), while for  $\nabla_S \zeta$ -terms cf. Remark 1 below. In (15h),  $\operatorname{div}_S := \operatorname{trace}(\nabla_S)$  denotes the  $(d-1)$ -dimensional ‘‘surface divergence’’. Furthermore, the flow rule (10) for  $\pi$  reads as:

$$|\sigma_t - \kappa_H \pi| \leq \sigma_{t,\text{yield}} \quad \text{with } \sigma_t = \zeta \kappa_t (\llbracket u \rrbracket_t - \pi), \quad (15i)$$

$$\dot{\pi} = \begin{cases} \lambda(\sigma_t - \kappa_H \pi), & \lambda \geq 0 \quad \text{if } |\sigma_t - \kappa_H \pi| = \sigma_{t,\text{yield}}, \\ 0 & \text{if } |\sigma_t - \kappa_H \pi| < \sigma_{t,\text{yield}}. \end{cases} \quad (15j)$$

Additionally, the following boundary conditions are imposed:

$$u = w_D \quad \text{on } \Gamma_D, \quad (15k)$$

$$\mathbb{C}e(u)\nu = 0 \quad \text{on } \Gamma_N, \quad (15l)$$

$$\nabla_S \zeta \cdot \tilde{\nu} = 0 \quad \text{on } \partial\Gamma_C, \quad (15m)$$

where  $\mathbb{C} = \mathbb{C}^{(i)}$  in (15l) with  $i$  referring to  $\Omega_i$  adjacent to a particular part of  $\Gamma_N$ ,  $\tilde{\nu}$  denotes the unit vector lying in  $\Gamma_C$  and being outward normal to  $\partial\Gamma_C$ .

**Remark 1.** The last term in (15h) involves  $(\operatorname{div}_S \nu)$  which is (up to a factor  $-\frac{1}{2}$ ) the mean curvature of the surface  $\Gamma_C$ , and it arises by applying a Green formula on a curved surface

$$\int_{\Gamma_C} w : ((\nabla_S \nu) \otimes \nu) \, dS = \int_{\Gamma_C} (\operatorname{div}_S \nu) (w : (\nu \otimes \nu)) \, v - \operatorname{div}_S (w \cdot \nu) \, v \, dS + \int_{\partial\Gamma_C} (w \cdot \tilde{\nu}) \, v \, dl \quad (16)$$

used with  $w = \kappa_0 |\nabla_S \zeta|^{r-2} \nabla_S \zeta$  and with the boundary condition  $w \cdot \tilde{\nu} = 0$  on  $\partial\Gamma_C$ , cf. (15m), for the directional-derivative term  $\int_{\Gamma_C} \kappa_0 |\nabla_S \zeta|^{r-2} \nabla_S \zeta \cdot \nabla_S \zeta \, dS$  arising from the term  $\int_{\Gamma_C} \frac{\kappa_0}{r} |\nabla_S \zeta|^r \, dS$  in (4a). Instead of scalar-valued  $\zeta$ , the vectorial variant of the Green-type identity (16) was used in a similar context in mechanics of complex (also called nonsimple) continua, cf. [17, 40, 55]. Of course, the boundary-value problem (15) is to be completed by the initial conditions, see (9) above. This quite complicated boundary-value problem will be, however, formulated and analysed in a much simpler and elegant, so-called energetic form in Sect. 3.

**Remark 2.** Note that,  $\zeta$  does not multiply the hardening term  $\frac{\kappa_H}{2} |\pi|^2$  in (4a) so that  $\kappa_H$  does not appear in (8). This can be ‘‘microscopically’’ interpreted that the energy spent in developing the hardening in the adhesive remains deposited in ‘‘microparticles’’ of the adhesive even after it completely disintegrates by ‘‘microcracks’’. Mathematically, it ensures coercivity on  $\mathcal{E}$  in  $L^2(\Gamma_C)$  with respect to  $\pi$ , while the alternative model, that would use the hardening term multiplied by  $\zeta$ , would exhibit only coercivity in  $L^1(\Gamma_C)$  (or rather in measures) via  $\mathcal{R}$  and, like in perfect plasticity, demanding mathematical techniques would be needed.

**3. Mathematical analysis of the model.** We will use the notation  $B([0, T]; \mathcal{U})$  for the Banach space of bounded measurable functions  $[0, T] \rightarrow \mathcal{U}$  defined everywhere, and  $BV([0, T]; \mathcal{X})$  for functions  $[0, T] \rightarrow \mathcal{X}$  with bounded variation. Recall that the variation of  $z : [0, T] \rightarrow \mathcal{X}$  is defined as  $\sup \sum_{j=1}^N \|z(t_j) - z(t_{j-1})\|$ , where  $\|\cdot\|$  is the norm on  $\mathcal{X}$  and the supremum is taken over all partitions of  $[0, T]$ . The philosophy of  $\mathcal{X} \supset \mathcal{Z}$  is denoting explicitly a Banach space on which  $\mathcal{R}$  is coercive in the sense that  $\mathcal{R}(z) \geq \varepsilon \|z\|$  for some  $\varepsilon > 0$ .

A fruitful concept of a certain weak solution to the doubly nonlinear inclusion with degree-1 homogeneous dissipation potential  $\mathcal{R}$ , called energetic solutions, was developed by Mielke et al. [27, 28, 30, 32, 34–36]. In the convex case, this concept is essentially equivalent to the conventional weak-solution concept, while in our case where  $\mathcal{E}(t, \cdot, \cdot)$  is non-convex this concept represents a generalization which is well amenable to mathematical analysis and numerical implementation and applicable to engineering problems, too.

**Definition 1** (Energetic solutions, [34, 35]). The process  $(u, z) : [0, T] \rightarrow \mathcal{U} \times \mathcal{Z}$  is called an energetic solution to the initial-value problem (1) given by  $(\mathcal{U} \times \mathcal{Z}, \mathcal{E}, \mathcal{R})$  and the initial condition  $(u_0, z_0)$  if  $u \in B([0, T]; \mathcal{U})$ , and  $z \in B([0, T]; \mathcal{Z}) \cap BV([0, T]; \mathcal{X})$ , and if

(i) the energy equality holds:

$$\underbrace{\mathcal{E}(T, u(T), z(T))}_{\text{stored energy at time } t=T} + \underbrace{\text{Diss}_{\mathcal{R}}(z, [0, T])}_{\text{energy dissipated during } [0, T]} = \underbrace{\int_0^T \mathcal{E}'_t(t, u, z) dt}_{\text{work done by mechanical load}} + \underbrace{\mathcal{E}(0, u_0, z_0)}_{\text{stored energy at time } t=0}, \quad (17)$$

where

$$\text{Diss}_{\mathcal{R}}(z, [0, T]) := \sup \sum_{j=1}^N \mathcal{R}(z(t_j) - z(t_{j-1})), \quad (18)$$

with the supremum taken over all partitions  $0 \leq t_0 < t_1 < \dots < t_{N-1} < t_N \leq T$ ,

(ii) the following *stability* inequality holds for any  $t \in [0, T]$ :

$$\forall (\tilde{u}, \tilde{z}) \in \mathcal{U} \times \mathcal{Z} : \quad \mathcal{E}(t, u, z) \leq \mathcal{E}(t, \tilde{u}, \tilde{z}) + \mathcal{R}(\tilde{z} - z), \quad (19)$$

(iii) the initial conditions  $u(0) = u_0$  and  $z(0) = z_0$  hold.

The definition of energetic solutions involves the time derivative of the stored energy, cf. (17), which is hardly defined for (4a) unless  $w_D$  is constant in time. Therefore, we need to transform the problem to avoid this rather technical difficulty. Using the additive shift  $u - u_D(t)$  with  $u_D$  being a suitable extension of the formerly defined boundary condition  $w_D$ , we obtain a problem with time-constant Dirichlet boundary conditions. Thus, up to an irrelevant time-dependent constant, (4a) transforms to

$$\tilde{\mathcal{E}}(t, u, \zeta, \pi) := \begin{cases} \sum_{i=1}^N \int_{\Omega_i} \mathbb{C}^{(i)} e(u) : e\left(\frac{u}{2} + u_D(t)\right) dx \\ + \int_{\Gamma_C} \left( \zeta \left( \frac{\kappa_n}{2} \|\llbracket u \rrbracket_n\|^2 + \frac{\kappa_t}{2} \|\llbracket u \rrbracket_t - \pi\|^2 \right) \right. \\ \left. + \frac{\kappa_H}{2} |\pi|^2 + \frac{\kappa_0}{r} |\nabla_S \zeta|^r \right) dS & \text{if } \llbracket u \rrbracket_n \geq 0, \quad 0 \leq \zeta \leq 1 \text{ on } \Gamma_C, \\ \infty & \text{elsewhere,} \end{cases} \quad (20)$$

while the homogeneous Dirichlet condition is incorporated in the underlying function space. More specifically, we use the function-spaces setting:

$$\mathcal{U} := \{u \in W^{1,2}(\Omega \setminus \Gamma_C; \mathbb{R}^d); u = 0 \text{ on } \Gamma_D\}, \quad (21a)$$

$$\mathcal{Z} := (L^\infty(\Gamma_C) \cap W^{1,r}(\Gamma_C)) \times L^2(\Gamma_C; \mathbb{R}^{d-1}), \quad (21b)$$

$$\mathcal{X} := L^1(\Gamma_C) \times L^1(\Gamma_C; \mathbb{R}^{d-1}). \quad (21c)$$

We will understand an energetic solution to the transformed problem determined by  $\tilde{\mathcal{E}}$  from (20) and  $\mathcal{R}$  from (4b), after the shift by  $u_D$  as a certain generalized energetic solution to the original problem determined by  $(\mathcal{E}, \mathcal{R})$  from (4), although Definition 1 cannot directly be applied to the

original problem, in contrast to the transformed problem,  $\tilde{\mathcal{E}}'_t$  occurring in (17) is now well defined and given by

$$\tilde{\mathcal{E}}'_t(t, u, \zeta, \pi) = \sum_{i=1}^N \int_{\Omega_i} \mathbb{C}^{(i)} e(u) : e(\dot{u}_D(t)) \, dx. \quad (22)$$

Further, we impose the following assumptions:

$$\mathbb{C}^{(i)} \text{ positive definite, symmetric, } \kappa_0, \kappa_H > 0, \quad \kappa_t, \kappa_n \geq 0, \quad a_1, \sigma_{t, \text{yield}} > 0, \quad (23a)$$

$$w_D \in W^{1,1}(0, T; W^{1/2,2}(\Gamma_D \cup \Gamma_0; \mathbb{R}^d)), \quad (23b)$$

$$(u_0, \zeta_0, \pi_0) \in W^{1,2}(\Omega \setminus \Gamma_C; \mathbb{R}^d) \times W^{1,r}(\Gamma_C) \times L^2(\Gamma_C; \mathbb{R}^{d-1}) \text{ stable at } t = 0. \quad (23c)$$

The condition (23c) means that  $\tilde{\mathcal{E}}(0, u_0, \zeta_0, \pi_0) \leq \tilde{\mathcal{E}}(0, \tilde{u}, \tilde{\zeta}, \tilde{\pi}) + \mathcal{R}(\tilde{\zeta} - \zeta_0, \tilde{\pi} - \pi_0)$  for all  $(\tilde{u}, \tilde{z}) \in \mathcal{U} \times \mathcal{Z}$ , where  $z = (\zeta, \pi)$  and  $\tilde{z} = (\tilde{\zeta}, \tilde{\pi})$ . The qualification (23b) allows for an extension  $u_D$  of  $w_D$  which belongs to  $W^{1,1}(0, T; W^{1,2}(\Omega; \mathbb{R}^d))$ ; in what follows, we will consider some extension with this property.

**Proposition 1** (Existence of energetic solutions). *Let  $r > d-1$ , and (2), and (23) hold. Then the problem determined by  $\tilde{\mathcal{E}}$  from (20), by  $\mathcal{R}$  from (4b), and by the initial conditions  $(u_0, z_0)$  possesses energetic solutions.*

*Proof.* For clarity, we will divide the proof into several steps (used quite standardly in the theory of rate-independent processes, cf. e.g. [27, 30]).

*Step 1 – approximate solution and a-priori estimates:* We make an implicit time discretisation by using, for simplicity, an equidistant partition of  $[0, T]$  with a time-step  $\tau > 0$ , assuming  $T/\tau \in \mathbb{N}$ . This is also referred to as a *Rothe method*, and leads to a recursive minimization problem

$$\left. \begin{array}{l} \text{minimize} \quad (u, z) \mapsto \tilde{\mathcal{E}}(k\tau, u, z) + \mathcal{R}(z - z_\tau^{k-1}) \\ \text{subject to} \quad (u, z) \in \mathcal{U} \times \mathcal{Z}, \end{array} \right\} \quad (24)$$

to be solved successively for  $k = 1, \dots, T/\tau$ , starting from  $u_\tau^0 = u_0$  and  $z_\tau^0 = z_0$ . By the standard direct method, existence of solutions to (24) is due to the weak sequential lower semicontinuity and coercivity of  $\tilde{\mathcal{E}}(t, \cdot, \cdot) + \mathcal{R}(\cdot - z_\tau^{k-1})$  in the space  $\mathcal{U} \times \mathcal{Z}$ .

Comparing the energy value of a solution at the level  $k$  with that of a solution  $(u_\tau^{k-1}, z_\tau^{k-1})$  of the incremental problem (24) at the level  $k-1$  gives  $\tilde{\mathcal{E}}(k\tau, u_\tau^k, z_\tau^k) + \mathcal{R}(z_\tau^k - z_\tau^{k-1}) \leq \tilde{\mathcal{E}}(k\tau, u_\tau^{k-1}, z_\tau^{k-1}) + \mathcal{R}(z_\tau^{k-1} - z_\tau^{k-2}) = \tilde{\mathcal{E}}(k\tau, u_\tau^{k-1}, z_\tau^{k-1})$ , which yields an upper estimate of the energy balance in the  $k^{\text{th}}$ -step:

$$\begin{aligned} & \tilde{\mathcal{E}}(k\tau, u_\tau^k, z_\tau^k) + \mathcal{R}(z_\tau^k - z_\tau^{k-1}) - \tilde{\mathcal{E}}((k-1)\tau, u_\tau^{k-1}, z_\tau^{k-1}) \\ & \leq \tilde{\mathcal{E}}(k\tau, u_\tau^{k-1}, z_\tau^{k-1}) - \tilde{\mathcal{E}}((k-1)\tau, u_\tau^{k-1}, z_\tau^{k-1}) = \int_{(k-1)\tau}^{k\tau} \tilde{\mathcal{E}}'_t(t, u_\tau^{k-1}, z_\tau^{k-1}) \, dt. \end{aligned} \quad (25)$$

From this, by using the coercivity/growth assumptions (23a) with (2), discrete Gronwall's inequality a-priori estimates can be derived. Namely, one gets

$$\|\bar{u}_\tau\|_{\mathbb{B}([0, T]; \mathcal{U})} \leq C, \quad (26a)$$

$$\|\bar{z}_\tau\|_{\mathbb{B}([0, T]; \mathcal{Z}) \cap \text{BV}([0, T]; \mathcal{Z})} \leq C, \quad (26b)$$

where  $\bar{u}_\tau$  and  $\bar{z}_\tau$  denote the piecewise constant interpolants defined as

$$\bar{u}_\tau(t) = u_\tau^k \quad \text{and} \quad \bar{z}_\tau(t) = z_\tau^k \quad \text{for } (k-1)\tau < t \leq k\tau, \quad k = 1, \dots, T/\tau. \quad (27)$$

*Step 2 – selection of convergent subsequences:* We further select convergent subsequences by using Banach and Helly principles; the latter one is used for the  $z$ -component which has a bounded variation. Using further the argument of strict convexity of  $\tilde{\mathcal{E}}(t, \cdot, z)$ , one shows that also the  $u$ -component converges at each time  $t$ . Thus we obtain:

$$\bar{u}_\tau(t) \rightarrow u(t) \quad \text{weakly in } \mathcal{U} \quad \text{for any } t \in [0, T], \quad (28a)$$

$$\bar{z}_\tau(t) \rightarrow z(t) \quad \text{weakly}^* \text{ in } \mathcal{Z} \quad \text{for any } t \in [0, T]. \quad (28b)$$

*Step 3 – stability:* Let us consider a solution  $(u_\tau^k, z_\tau^k) \in \mathcal{U} \times \mathcal{Z}$  of the incremental problem (24) at the level  $k$  and compare its energy value with the one of an arbitrary  $(\tilde{u}, \tilde{z})$ . We obtain the discrete stability:

$$\tilde{\mathcal{E}}(k\tau, u_\tau^k, z_\tau^k) \leq \tilde{\mathcal{E}}(k\tau, \tilde{u}, \tilde{z}) + \mathcal{R}(\tilde{z} - z_\tau^{k-1}) - \mathcal{R}(z_\tau^k - z_\tau^{k-1}) \leq \tilde{\mathcal{E}}(k\tau, \tilde{u}, \tilde{z}) + \mathcal{R}(\tilde{z} - z_\tau^k) \quad (29)$$

where we used that  $\mathcal{R}$  satisfies the triangle inequality  $\mathcal{R}(\tilde{z} - z_\tau^{k-1}) \leq \mathcal{R}(z_\tau^k - z_\tau^{k-1}) + \mathcal{R}(\tilde{z} - z_\tau^k)$  due to its degree-1 homogeneity.

For the passage to the limit from (29) to (19), it was identified in [32] that one needs to find, for any stable sequence  $\{(t_j, u_j, z_j)\}_{j \in \mathbb{N}}$  converging weakly in  $[0, T] \times \mathcal{U} \times \mathcal{Z}$  to some  $(t, u, z)$  and for any  $(\tilde{u}, \tilde{z}) \in \mathcal{U} \times \mathcal{Z}$ , a so-called mutual recovery sequence  $(\tilde{u}_j, \tilde{z}_j)_{j \in \mathbb{N}}$  such that

$$\limsup_{j \rightarrow \infty} \tilde{\mathcal{E}}(t_j, \tilde{u}_j, \tilde{z}_j) + \mathcal{R}(\tilde{z}_j - z_j) - \tilde{\mathcal{E}}(t_j, u_j, z_j) \leq \tilde{\mathcal{E}}(t, \tilde{u}, \tilde{z}) + \mathcal{R}(\tilde{z} - z) - \tilde{\mathcal{E}}(t, u, z). \quad (30)$$

We used only stable sequences, i.e. such sequences  $\{(t_j, u_j, z_j)\}_{j \in \mathbb{N}}$  that  $\sup_{j \in \mathbb{N}} \tilde{\mathcal{E}}(t_j, u_j, z_j) < \infty$  and  $\tilde{\mathcal{E}}(t_j, u_j, z_j) \leq \tilde{\mathcal{E}}(t_j, \tilde{u}, \tilde{z}) + \mathcal{R}(\tilde{z} - z_j)$  for all  $(\tilde{u}, \tilde{z}) \in \mathcal{U} \times \mathcal{Z}$ , because other sequences never come into competition.

To verify (30), we can combine the damage-type construction for  $\zeta$  (cf. [29]) and the so-called binomial trick for  $\pi$ . More specifically, we put

$$\tilde{u}_j := \tilde{u}, \quad (31a)$$

$$\tilde{\zeta}_j := (\tilde{\zeta} - \|\zeta_j - \zeta\|_{L^\infty(\Gamma_C)})^+, \quad (31b)$$

$$\tilde{\pi}_j := \tilde{\pi} + \pi_j - \pi, \quad (31c)$$

where  $(\cdot)^+$  denotes the positive part. Note that, by (31b) and by  $r > d-1$ , we have

$$0 \leq \tilde{\zeta}_j \leq \zeta_j \quad \text{a.e. on } \Gamma_C \quad \text{and} \quad \tilde{\zeta}_j \rightarrow \tilde{\zeta} \quad \text{in } W^{1,r}(\Gamma_C); \quad (32)$$

here  $\tilde{\zeta}_j \leq \zeta_j$  follows by  $\tilde{\zeta}_j = (\tilde{\zeta} - \|\zeta_j - \zeta\|_{L^\infty(\Gamma_C)})^+ \leq (\zeta - \|\zeta_j - \zeta\|_{L^\infty(\Gamma_C)})^+ \leq \zeta_j$ , where we used  $\zeta - \tilde{\zeta} \geq 0$  a.e. on  $\Gamma_C$  (otherwise  $\mathcal{R}(\tilde{z} - z) = \infty$  and (30) is satisfied trivially) and eventually also  $\zeta_j - \zeta \geq -\|\zeta_j - \zeta\|_{L^\infty(\Gamma_C)}$ . Moreover, we will use that (31c) yields

$$\tilde{\pi}_j - \pi_j = \tilde{\pi} - \pi \quad \text{and} \quad \tilde{\pi}_j \rightarrow \pi \quad \text{weakly in } L^2(\Gamma_C; \mathbb{R}^{d-1}). \quad (33)$$

Note that, in particular  $\tilde{\pi}_j - \pi_j$  is independent of  $j$ . In view of (20) and (4b), we have

$$\begin{aligned} & \tilde{\mathcal{E}}(t_j, \tilde{u}_j, \tilde{z}_j) + \mathcal{R}(\tilde{z}_j - z_j) - \tilde{\mathcal{E}}(t_j, u_j, z_j) \\ &= \sum_{i=1}^N \int_{\Omega_i} \mathbb{C}^{(i)} e(\tilde{u}_j) : e\left(\frac{\tilde{u}_j}{2} + u_D(t_j)\right) - \mathbb{C}^{(i)} e(u_j) : e\left(\frac{u_j}{2} + u_D(t_j)\right) dx \\ & \quad + \int_{\Gamma_C} \tilde{\zeta}_j \frac{\kappa_n}{2} |[\![\tilde{u}_j]\!]_n|^2 - \zeta_j \frac{\kappa_n}{2} |[\![u_j]\!]_n|^2 dS \\ & \quad + \int_{\Gamma_C} \tilde{\zeta}_j \frac{\kappa_t}{2} |[\![\tilde{u}_j]\!]_t - \tilde{\pi}_j|^2 - \zeta_j \frac{\kappa_t}{2} |[\![u_j]\!]_t - \pi_j|^2 dS \\ & \quad + \int_{\Gamma_C} \frac{\kappa_H}{2} |\tilde{\pi}_j|^2 + \frac{\kappa_0}{r} |\nabla_S \tilde{\zeta}_j|^r - \frac{\kappa_H}{2} |\pi_j|^2 - \frac{\kappa_0}{r} |\nabla_S \zeta_j|^r dS \\ & \quad + \int_{\Gamma_C} a_1 |\tilde{\zeta}_j - \zeta_j| + \sigma_{t,\text{yield}} |\tilde{\pi}_j - \pi_j| dS \\ & =: I_j^{(1)} + I_j^{(2)} + I_j^{(3)} + I_j^{(4)} + I_j^{(5)}. \end{aligned} \quad (34)$$

Let us emphasize that we used  $0 \leq \tilde{\zeta}_j \leq \zeta_j \leq 1$  to comply with the constraints involved in both (20) with irreversibility contained in (4b). Let us discuss the particular terms. For  $I_j^{(1)}$ , we can just use concavity and thus weak upper semicontinuity of  $u_j \mapsto \int_{\Omega_i} -\mathbb{C}^{(i)} e(u_j) : e(\frac{1}{2}u_j + u_D(t_j)) dx$

so that

$$\begin{aligned} \limsup_{j \rightarrow \infty} I_j^{(1)} &= \limsup_{j \rightarrow \infty} \sum_{i=1}^N \int_{\Omega_i} \mathbb{C}^{(i)} e(\tilde{u}):e\left(\frac{\tilde{u}}{2}+u_D(t_j)\right) - \mathbb{C}^{(i)} e(u_j):e\left(\frac{u_j}{2}+u_D(t_j)\right) dx \\ &\leq \sum_{i=1}^N \int_{\Omega_i} \mathbb{C}^{(i)} e(\tilde{u}):e\left(\frac{\tilde{u}}{2}+u_D(t)\right) - \mathbb{C}^{(i)} e(u):e\left(\frac{u}{2}+u_D(t)\right) dx. \end{aligned} \quad (35)$$

The convergence of the integral  $I_j^{(2)}$  is simple because, by compactness of the trace operator  $u \mapsto \llbracket u \rrbracket : W^{1,2}(\Omega \setminus \Gamma_C; \mathbb{R}^d) \rightarrow L^2(\Gamma_C; \mathbb{R}^d)$ , we have the strong convergence  $\|\llbracket u_j \rrbracket_n\|^2 \rightarrow \|\llbracket u \rrbracket_n\|^2$  in  $L^1(\Gamma_C)$ . Further, we can estimate

$$\begin{aligned} \limsup_{j \rightarrow \infty} I_j^{(3)} &= \frac{1}{2} \lim_{j \rightarrow \infty} \int_{\Gamma_C} \tilde{\zeta}_j \kappa_t (\llbracket \tilde{u}_j - u_j \rrbracket_t - \tilde{\pi}_j + \pi_j) \cdot (\llbracket \tilde{u}_j + u_j \rrbracket_t - \tilde{\pi}_j - \pi_j) dS \\ &\quad - \frac{1}{2} \liminf_{j \rightarrow \infty} \int_{\Gamma_C} (\zeta_j - \tilde{\zeta}_j) \kappa_t |\llbracket u_j \rrbracket_t - \pi_j|^2 dS \\ &= \frac{1}{2} \lim_{j \rightarrow \infty} \int_{\Gamma_C} \tilde{\zeta}_j \kappa_t (\llbracket \tilde{u} - u_j \rrbracket_t - \tilde{\pi} + \pi) \cdot (\llbracket \tilde{u}_j + u_j \rrbracket_t - \tilde{\pi}_j - \pi_j) dS \\ &\quad - \frac{1}{2} \liminf_{j \rightarrow \infty} \int_{\Gamma_C} (\zeta - \tilde{\zeta}) \kappa_t |\llbracket u_j \rrbracket_t - \pi_j|^2 dS \\ &\quad + \frac{1}{2} \lim_{j \rightarrow \infty} \int_{\Gamma_C} (\zeta - \tilde{\zeta} - \zeta_j + \tilde{\zeta}_j) \kappa_t |\llbracket u_j \rrbracket_t - \pi_j|^2 dS \\ &\leq \frac{1}{2} \int_{\Gamma_C} \tilde{\zeta} \kappa_t (\llbracket \tilde{u} - u \rrbracket_t - \tilde{\pi} + \pi) \cdot (\llbracket \tilde{u} + u \rrbracket_t - \tilde{\pi} - \pi) + (\tilde{\zeta} - \zeta) \kappa_t |\llbracket u \rrbracket_t - \pi|^2 dS \\ &= \frac{1}{2} \int_{\Gamma_C} \tilde{\zeta} \kappa_t |\llbracket \tilde{u} \rrbracket_t - \tilde{\pi}|^2 - \zeta \kappa_t |\llbracket u \rrbracket_t - \pi|^2 dS \end{aligned} \quad (36)$$

where we also used that  $\zeta - \tilde{\zeta} \geq 0$  so that the functional  $\int_{\Gamma_C} (\zeta - \tilde{\zeta}) \kappa_t |\cdot|^2 dS$  is convex and thus weakly lower semicontinuous on  $L^2(\Gamma_C; \mathbb{R}^{d-1})$ , and that  $\zeta - \tilde{\zeta} - \zeta_j + \tilde{\zeta}_j \rightarrow 0$  strongly in  $L^\infty(\Gamma_C)$  while  $\|\llbracket u_j \rrbracket_t - \pi_j\|^2$  is bounded in  $L^1(\Gamma_C)$  so that  $(\zeta - \tilde{\zeta} - \zeta_j + \tilde{\zeta}_j) \kappa_t |\llbracket u_j \rrbracket_t - \pi_j|^2$  converges to zero in  $L^1(\Gamma_C)$ . Further, it obviously holds that

$$\limsup_{j \rightarrow \infty} I_j^{(4)} \leq \int_{\Gamma_C} \frac{\kappa_H}{2} |\tilde{\pi}|^2 + \frac{\kappa_0}{r} |\nabla_S \tilde{\zeta}|^r - \frac{\kappa_H}{2} |\pi|^2 - \frac{\kappa_0}{r} |\nabla_S \zeta|^r dS. \quad (37)$$

In (37) we have used the strong convergence (32), and another binomial trick now for

$$|\tilde{\pi}_j|^2 - |\pi_j|^2 = (\tilde{\pi}_j - \pi_j) \cdot (\tilde{\pi}_j + \pi_j) = (\tilde{\pi} - \pi) \cdot (\tilde{\pi}_j + \pi_j) \rightarrow (\tilde{\pi} - \pi) \cdot (\tilde{\pi} + \pi) = |\tilde{\pi}|^2 - |\pi|^2$$

weakly in  $L^1(\Gamma_C)$  due to (33), and also the weak upper semicontinuity of the concave functional  $\zeta \mapsto \int_{\Gamma_C} -\frac{\kappa_0}{r} |\nabla_S \zeta|^r dS$  used for the last term in (37). Eventually, we have

$$\lim_{j \rightarrow \infty} I_j^{(5)} = \lim_{j \rightarrow \infty} \int_{\Gamma_C} a_1 |\tilde{\zeta}_j - \zeta_j| + \sigma_{t,\text{yield}} |\tilde{\pi}_j - \pi_j| dS = \int_{\Gamma_C} a_1 |\tilde{\zeta} - \zeta| + \sigma_{t,\text{yield}} |\tilde{\pi} - \pi| dS \quad (38)$$

due to both (32) and (33), and also due to the compact embedding  $W^{1,r}(\Gamma_C) \Subset L^1(\Gamma_C)$  so that  $\zeta_j \rightarrow \zeta$  strongly in  $L^1(\Gamma_C)$ . Altogether, (30) was proved.

*Step 4 - upper energy inequality:* Summing (25) for  $k = 1, \dots, t/\tau \in \mathbb{N}$  and denoting by  $\underline{u}_\tau$  and  $\underline{z}_\tau$  the “delayed” piecewise constant interpolants defined as

$$\underline{u}_\tau(t) = u_\tau^{k-1} \quad \text{and} \quad \underline{z}_\tau(t) = z_\tau^{k-1} \quad \text{for} \quad (k-1)\tau < t \leq k\tau, \quad k = 1, \dots, T/\tau, \quad (39)$$

we arrive at

$$\tilde{\mathcal{E}}(s, \bar{u}_\tau(t), \bar{z}_\tau(t)) + \text{Diss}_{\mathcal{R}}(\bar{z}_\tau, [0, t]) - \tilde{\mathcal{E}}(0, u_0, z_0) \leq \int_0^t \tilde{\mathcal{E}}'_t(s, \underline{u}_\tau(s), \underline{z}_\tau(s)) ds. \quad (40)$$

Actually, we will use it for  $t = T$  in this proof. The passage to the limit in the left-hand side of (40) is by weak lower-semicontinuity, while

$$\tilde{\mathcal{E}}'_t(\underline{u}_\tau, \underline{z}_\tau) = \sum_{i=1}^N \int_{\Omega_i} \mathbb{C}^{(i)} e(\underline{u}_\tau):e(\dot{u}_D(t)) dx \rightarrow \sum_{i=1}^N \int_{\Omega_i} \mathbb{C}^{(i)} e(u):e(\dot{u}_D(t)) dx = \tilde{\mathcal{E}}'_t(u, z) \quad (41)$$

in  $L^1(0, T)$  can be proved. Convergence (41) follows from (22) and the fact that  $e(\underline{u}_r) \rightarrow e(u)$  weakly\* in  $L^\infty(0, T; L^2(\Omega; \mathbb{R}^{d \times d}))$ .

*Step 5 – lower energy inequality.* The opposite inequality in (40) can be proved by the well-known trick based on the approximation of the Lebesgue integral by Riemann sums, using the already proved stability (19) and also the stability of the initial condition (23c), cf. [11, 27].  $\square$

**Remark 3** (Alternative models). Our simple construction (31) relied on the embedding  $W^{1,r}(\Gamma_C) \subset C(\bar{\Gamma}_C)$  which holds for  $r > d-1$ , and simplifies the mathematical analysis in this paper. For  $1 < r \leq d-1$  and  $r = 1$ , respectively, one would have to use the sophisticated construction from [51, 53] and [52]. Alternatively, one can avoid gradient theory for  $\zeta$  if one considers gradient theory for  $\pi$ , i.e. instead of the stored energy  $\sum_{i=1}^N \int_{\Omega_i} \mathbb{C}^{(i)} e(u) : e(\frac{1}{2}u + u_D(t)) \, dx + \int_{\Gamma_C} \zeta (\kappa_n |\llbracket u \rrbracket_n|^2 + \kappa_t |\llbracket u \rrbracket_t - \pi|^2) + \kappa_H |\pi|^2 + \frac{\kappa_0}{r} |\nabla_S \zeta|^r \, dS$ , one can consider

$$\begin{aligned} & \sum_{i=1}^N \int_{\Omega_i} \mathbb{C}^{(i)} e(u) : e(\frac{u}{2} + u_D(t)) \, dx \\ & + \int_{\Gamma_C} \zeta (\kappa_n |\llbracket u \rrbracket_n|^2 + \kappa_t |\llbracket u \rrbracket_t - \pi|^2) + \kappa_H |\pi|^2 + \frac{\kappa_0}{2} |\nabla_S \pi|^2 \, dS. \end{aligned} \quad (42)$$

Relying on the quadratic form of the last term, a specific construction of a mutual recovery sequence for (30) can combine the ideas from [46] for  $\zeta$  with the binomial trick for  $u$  and  $\pi$ . Namely,

$$\tilde{u}_j := \tilde{u}, \quad (43a)$$

$$\tilde{\zeta}_j := \begin{cases} \zeta_j \tilde{\zeta} / \zeta & \text{wherever } \zeta \geq 0, \\ 0 & \text{otherwise,} \end{cases} \quad (43b)$$

$$\tilde{\pi}_j := \tilde{\pi} + \pi_j - \pi. \quad (43c)$$

Instead of (32), we have

$$0 \leq \tilde{\zeta}_j \leq \zeta_j \text{ a.e. on } \Gamma_C \text{ and } \tilde{\zeta}_j \rightarrow \tilde{\zeta} \text{ weakly* in } L^\infty(\Gamma_C). \quad (44)$$

Only slight changes in the argumentation in the proof of Proposition 1 are needed: (36) should use strong convergence of  $\pi_j$  and  $\tilde{\pi}_j$  while the modification of (37) should again use the binomial trick in terms of  $\pi$ -variable. The absence of the gradient of  $\zeta$  would facilitate the so-called Griffith-type behaviour, namely that  $\zeta(t, x)$  is valued only in  $\zeta_0(x)$  or 0, cf. [31, 51].

**4. Illustrative example and validation of the model.** The main purpose of this section is to demonstrate on a 2-dimensional example that the proposed model indeed produces solutions that delaminate the adhesive surface with the fracture-activation energy increased in mixed-mode, which is not entirely a-priori obvious.

**4.1. Geometry of a two-dimensional example.** The geometry of the problem is shown in Fig. 3. With reference to Fig. 1, only one subdomain (i.e.  $N = 1$ ) is used.

A time-dependent Dirichlet boundary condition (in engineering literature also referred to as hard-device loading) is assumed by imposing at the right-hand side  $\Gamma_D$  of the rectangle  $\partial\Omega$  a prescribed horizontal and vertical displacements, respectively,  $w_x$  and  $w_y = 0.6w_x$ . All the other boundary parts, defining the Neumann boundary  $\Gamma_N$ , except of the contact surface  $\Gamma_C$ , are considered to be traction free. The Dirichlet loading is assumed to increase linearly in time, being motivated by the pull-push shear experimental test used in engineering practice [10].

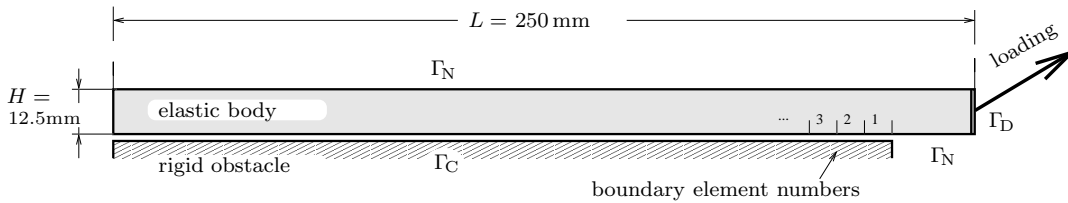


Fig. 3. Geometry and boundary conditions of the problem considered. The length of the initially glued part  $\Gamma_C$  is  $0.9L = 225$  mm.

**4.2. Material of the bulk and of the adhesive.** We consider an isotropic elastic material in the bulk, i.e.  $\mathbb{C}_{ijkl} = \lambda\delta_{ij}\delta_{kl} + \mu(\delta_{ik}\delta_{jl} + \delta_{il}\delta_{jk})$ , with the Lamé constants  $\lambda = \frac{\nu E}{(1+\nu)(1-2\nu)}$ , shear modulus  $\mu = \frac{E}{2(1+\nu)}$ , and Young's modulus  $E = 70$  GPa and Poisson's ratio  $\nu = 0.35$  (which corresponds to aluminium). Elastic plain strain states, with unit thickness, are considered. For the adhesive a normal stiffness  $\kappa_n = 150$  GPa/m, a tangential stiffness with  $\kappa_t = \kappa_n/2$ , and the mode I fracture toughness  $a_I = 187.5$  J/m<sup>2</sup> are chosen. The critical stress for the normal direction is defined by  $\sigma_{n,crit} = \sqrt{2\kappa_n a_I}$ , while in the tangential direction  $\sigma_{t,yield} = 0.56\sigma_{n,crit}$ . In particular,  $\sigma_{n,crit} = 7.5$  MPa, while  $\sqrt{2\kappa_t a_I} = 5.3$  MPa. The condition (14) here means  $2.65 \text{ MPa} < \sigma_{t,yield} < 5.3 \text{ MPa}$  and is indeed satisfied since  $\sigma_{t,yield} = 0.56\sqrt{2\kappa_n a_I} = 0.56\sqrt{4\kappa_t a_I} \cong 4.2 \text{ MPa}$ . For the case with an interface-plastic slip the hardening slope is  $\kappa_H = \kappa_t/9$ . By (11c), this yields  $a_{II} \cong a_I + 556.1 \text{ J/m}^2 \cong 743.6 \text{ J/m}^2$ . By (13), we have the fracture-mode sensitivity  $a_{II}/a_I \cong 4$ .

**4.3. Computational implementation.** The implicit time-discretisation used for analysis in Section 3 gives also a conceptual numerical strategy, namely to solve the recursive minimization problem (24) after making a spatial discretisation, cf. [30].

A common numerical technique utilized for this goal is the finite element method (FEM), see e.g. [23, 33]. However, as also noticed in [45], in the delamination problems we may only be interested in the traces of displacements (and tractions) on the boundaries  $\partial\Omega_i$ . Thus, it would be desirable to eliminate all the unknowns associated to the interior points in  $\Omega_i$ . This suggests to utilize the boundary element method (BEM) in order to solve separately the boundary value problems defined on elastic subdomains  $\Omega_i$ .

We use the discretisation of  $\Gamma_C$  by the boundary element mesh of 30 elements of equal length for horizontal sides and 2 elements along each vertical side. Thus,  $\Gamma_C$  consists of 27 elements of the length  $L_e \cong 8.33\text{mm}$ .

The alternating minimization algorithm proposed in [9] and a heuristic back-tracking algorithm proposed in [33] was then used for the global optimisation problem arising by the above outlined discretisation from (24).

Some numerical shortcuts comparing to the analysis presented in Sect. 3 have, however, been made: namely we neglected the gradient of  $\zeta$  and allowed for an additional discretisation error by implementing the boundary semi-discretisation by the conventional collocation BEM in a standard mixed formulation (i.e. involving also tractions). More specifically, we use a two-dimensional BEM code [38] employing continuous piecewise linear boundary elements [39]. cf. [26] for details.

**4.4. Computational experiments.** We present selected results obtained with the delamination test on the above described specimen subjected to increasing load with a constant speed until a complete delamination is achieved. The total number of 101 time steps solved corresponds to an increase of the prescribed displacements,  $w_x$ , from zero to the maximum value 0.1184 mm.

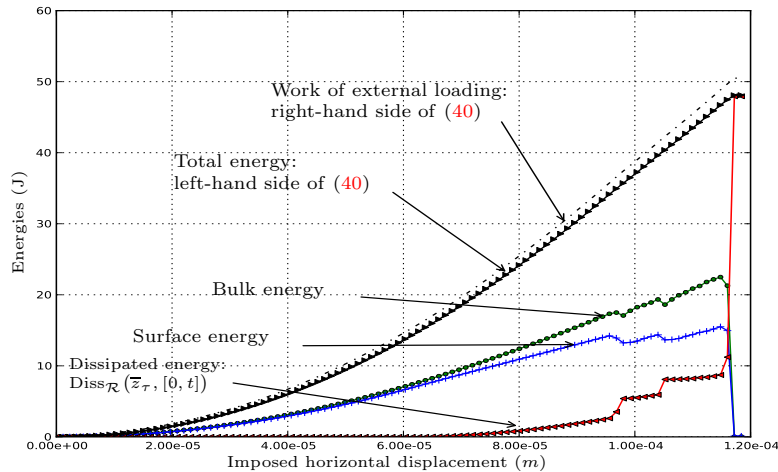


Fig. 4. Evolution of the energies in time, depicted in dependence of the displacement imposed in the horizontal direction  $w_x$  until complete rupture.

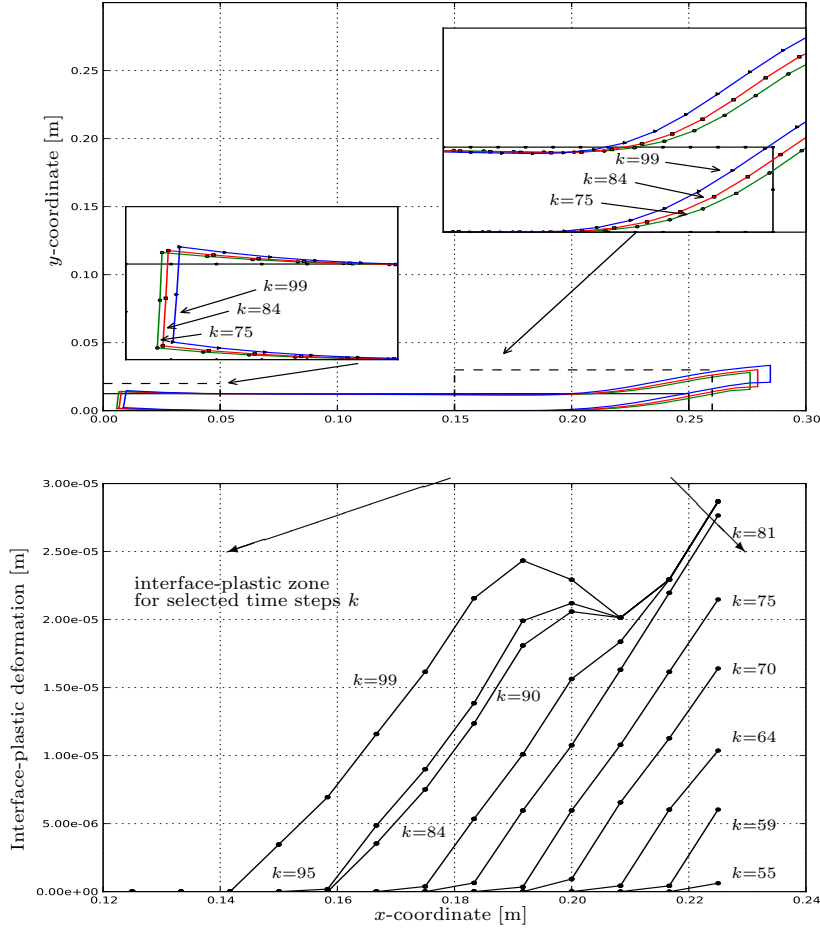


Fig. 5 Upper: Deformed elastic domain for 3 selected time steps  $k$  (displayed with the displacements magnified 100x) and a delamination tip zone (in mixed-mode) and also in the opposite end (in mode I) zoomed in.

Lower: Evolution of the interface-plastic slip depicted on the part of  $\Gamma_C$  which delaminates in mixed-mode for selected time steps  $k$ .

The energetics of the delamination process obtained for this case is shown in Fig. 4. After the delamination of some elements, suddenly the rest of the elements along  $\Gamma_C$  break in one time step. In fact, such a spontaneous-rupture behaviour might be expected, as in a related pull-push shear test a similar behaviour corresponding to a snap-back instability can be observed [10].

As expected, an interface-plastic zone appears ahead of the crack tip at the end of the delaminated zone. The value of the interface-plastic slip at a point ahead of the crack tip is increasing until the adhesive at this point is broken afterwards the interface-plastic slip therein remains constant. This can be seen in Fig. 5(lower), where the interface-plastic slip is plotted for various time steps  $k$ . The (scaled) deformed shape of the elastic domain  $\Omega$  is plotted in Fig. 5(upper) for the some of these time steps.

In Fig. 6 it is shown that an interface-plastic slip takes place at the nodes before a debonding happens. After the debonding takes place, at a node, the whole energy dissipated at this element remains constant. It is clear now that the dissipated energy takes values higher than the dissipated energy needed for delamination in opening mode I given by  $a_1$ . This can be observed in Fig. 7, where the ratio  $r$  of the accumulated dissipated energy on each element (up to the total delamination of the adhesive zone  $\Gamma_C$ ) to the mode I energy  $a_1 L_e$  is plotted.

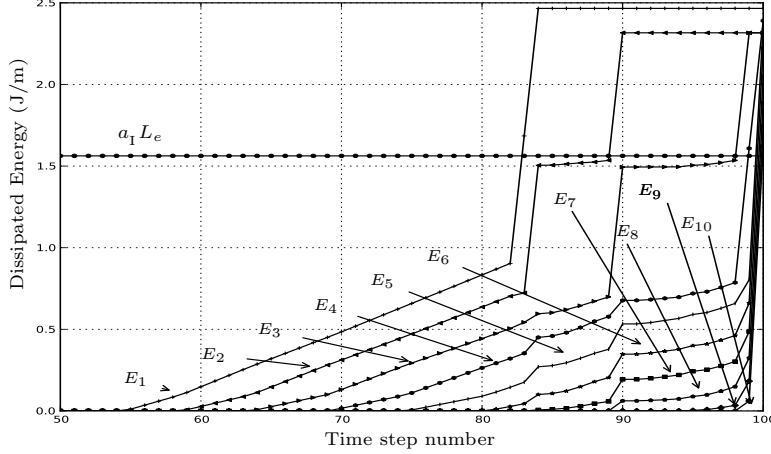


Fig. 6. Dissipated energy on elements  $E_1$  to  $E_{10}$ ; for comparison,  $a_1 L_e$  (=the energy needed for total break in mode I per length  $L_e$ ) is depicted, too. Nearly all these elements eventually exceed  $a_1 L_e$  so that they delaminate in mixed-mode.

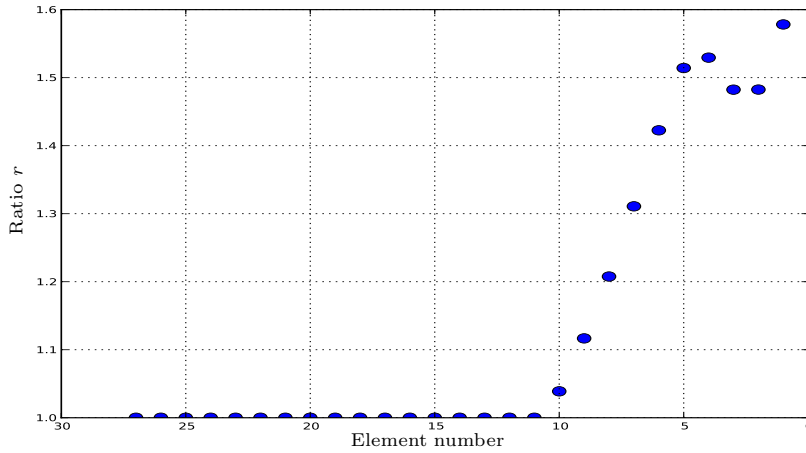


Fig. 7. Ratio  $r$  of the dissipated energy on each element to the mode-I energy  $a_I$  resulted at the end after its complete delamination; in view of  $a_{II}/a_I = 3.97$ , the right-end part was delaminated in mixed-mode combining about 80% mode I and 20% mode II, while the rest ruptured gradually (in the left end of the specimen as displayed in Fig. 5–upper) or spontaneously (in the middle part of the specimen) in pure mode I.

Finally, just for comparison, we also performed the same experiment but with interface-plasticity suppressed, i.e.  $\pi \equiv 0$ , so that modes I and II coincide with each other. This can be done simply just by putting the activation threshold  $\sigma_{t,yield}$  very large. This model was already treated both theoretically and computationally in [23]. The analog of Fig. 6 is presented in Fig. 8 where one can observe rather continuously propagating Griffith-type rupture, i.e. most elements are either fully bonded or fully debonded; in fact, it can be observed rather in the nodes than in the elements themselves, which is reflected by the occurrence of the mid-horizontal segments in Fig. 8. For the infinite stiffnesses of the adhesive (i.e. both  $\kappa_n \rightarrow \infty$  and  $\kappa_t \rightarrow \infty$ ), this Griffith-like response (i.e.  $\zeta$  taking values either 1 or 0 a.e.) can even rigorously be proved, cf. [51, Prop.4.3.3] or [31, Prop.4.4]. For finite (but large)  $\kappa_n$  and  $\kappa_t$ , this tendency is thus not surprising, cf. also the mentioned previous experiments in [23].

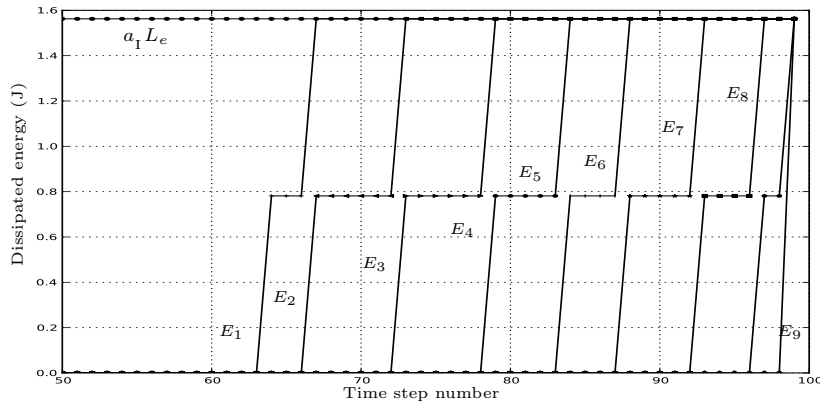


Fig. 8. Comparison with Fig. 6 if interface-plasticity is suppressed so that mode II dissipates equally as mode I and the dissipated energy, depicted on elements  $E_1$  to  $E_9$ , cannot exceed  $a_1 L_e$ .

## REFERENCES

- [1] E. C. Aifantis. On the microstructural origin of certain inelastic models. *ASME J. Eng. Mater. Technol.*, 106:326–330, 1984.
- [2] L. Banks-Sills and D. Askenazi. A note on fracture criteria for interface fracture. *Intl. J. Fracture*, 103:177–188, 2000.
- [3] Z. Bažant and M. Jirásek. Nonlocal integral formulations of plasticity and damage: Survey of progress. *J. Engng. Mech.*, 128(11):1119–1149, 2002.
- [4] S. Bennati, M. Colleluori, D. Corigliano, and P. Valvo. An enhanced beam-theory model of the asymmetric double cantilever beam (adcb) test for composite laminates. *Composites Science and Technology*, 69:1735–1745, 2009.
- [5] M. A. Biot. Thermoelasticity and irreversible thermodynamics. *J. Appl. Phys.*, 27:240–253, 1956.
- [6] M. A. Biot. *Mechanics of Incremental Deformations*. Wiley, New York, 1965.
- [7] E. Bonetti, G. Bonfanti, and R. Rossi. Well-posedness and long-time behaviour for a model of contact with adhesion. *Indiana Univ. Math. J.*, 56:2787–2820, 2007.
- [8] E. Bonetti, G. Bonfanti, and R. Rossi. Global existence for a contact problem with adhesion. *Math. Meth. Appl. Sci.*, 31:1029–1064, 2008.
- [9] B. Bourdin, G. A. Francfort, and J.-J. Marigo. Numerical experiments in revisited brittle fracture. *J. Mech. Phys. Solids*, 48:797–826, 2000.
- [10] P. Cornetti and A. Carpinteri. Modelling the FRP-concrete delamination by means of an exponential softening law. *Engineering Structures*, 33:1988–2001, 2011.
- [11] G. Dal Maso, G. Francfort, and R. Toader. Quasistatic crack growth in nonlinear elasticity. *Arch. Rational Mech. Anal.*, 176:165–225, 2005.
- [12] A. Evans, M. Rühle, B. Dalgleish, and P. Charalambides. The fracture energy of bimaterial interfaces. *Metallurgical Transactions A*, 21A:2419–2429, 1990.
- [13] M. Frémond. Dissipation dans l’adhérence des solides. *C.R. Acad. Sci., Paris, Sér. II*, 300:709–714, 1985.
- [14] M. Frémond. Contact with adhesion. In J. Moreau and G. Panagiotopoulos, editors, *Topics in Nonsmooth Mechanics*. Birkhäuser, 1988.
- [15] M. Frémond. *Non-Smooth Thermomechanics*. Springer-Verlag, Berlin, 2002.
- [16] M. Frémond and B. Nedjar. Damage, gradient of damage and principle of virtual power. *Internat. J. Solids Structures*, 33:1083–1103, 1996.
- [17] E. Fried and M. Gurtin. Traction, balances, and boundary conditions for nonsimple materials with application to liquid flow at small-length scales. *Arch. Rational Mech. Anal.*, 182:513–554, 2006.
- [18] A. Griffith. The phenomena of rupture and flow in solids. *Philos. Trans. Royal Soc. London Ser. A. Math. Phys. Eng. Sci.*, 221:163–198, 1921.
- [19] W. Han and B. D. Reddy. *Plasticity (Mathematical Theory and Numerical Analysis)*. Springer-Verlag, New York, 1999.
- [20] J. W. Hutchinson and Z. Suo. Mixed mode cracking in layered materials. *Advances in Applied Mechanics*, 29:63–191, 1992.
- [21] M. Jirásek and J. Zeman. Localization study of non-local energetic damage model. *ArXiv e-prints (no: 0804.3440v1)*, 2008.
- [22] D. Knees, A. Mielke, and C. Zanini. On the inviscid limit of a model for crack propagation. *Math. Models Meth. Appl. Sci. (M<sup>3</sup>AS)*, 18:1529–1569, 2008.
- [23] M. Kočvara, A. Mielke, and T. Roubíček. A rate-independent approach to the delamination problem. *Math. Mechanics Solids*, 11:423–447, 2006.
- [24] K. Liechti and Y. Chai. Asymmetric shielding in interfacial fracture under in-plane shear. *J. Appl. Mech.*, 59:295–304, 1992.

- [25] V. Mantič. Discussion on the reference length and mode mixity for a bimaterial interface. *J. Engr. Mater. Technology*, 130:045501–1–2, 2008.
- [26] V. Mantič, C. Panagiotopoulos, and T. Roubíček. Associative quasistatic mixed-mode delamination model and its BEM implementation. In preparation.
- [27] A. Mielke. Evolution in rate-independent systems (Ch. 6). In C. Dafermos and E. Feireisl, editors, *Handbook of Differential Equations, Evolutionary Equations, vol. 2*, pages 461–559. Elsevier B.V., Amsterdam, 2005.
- [28] A. Mielke. Differential, energetic and metric formulations for rate-independent processes. In L. Ambrosio and G. Savaré, editors, *Nonlinear PDEs and Applications*, pages 87–170. Springer, 2010.
- [29] A. Mielke and T. Roubíček. Rate-independent damage processes in nonlinear elasticity. *Math. Models Meth. Appl. Sci.*, 16:177–209, 2006.
- [30] A. Mielke and T. Roubíček. Numerical approaches to rate-independent processes and applications in inelasticity. *Math. Model. Numer. Anal. (M2AN)*, 43:399–428, 2009.
- [31] A. Mielke, T. Roubíček, and M. Thomas. From damage to delamination in nonlinearly elastic materials at small strains. *J. Elasticity*, 2010. Submitted. WIAS preprint 1542.
- [32] A. Mielke, T. Roubíček, and U. Stefanelli.  $\Gamma$ -limits and relaxations for rate-independent evolutionary problems. *Calc. Var. Part. Diff. Eqns.*, 31:387–416, 2008.
- [33] A. Mielke, T. Roubíček, and J. Zeman. Complete damage in elastic and viscoelastic media and its energetics. *Computer Methods Appl. Mech. Engr.*, 199:1242–1253, 2009.
- [34] A. Mielke and F. Theil. A mathematical model for rate-independent phase transformations with hysteresis. In H.-D. Alber, R. Balean, and R. Farwig, editors, *Proceedings of the Workshop on “Models of Continuum Mechanics in Analysis and Engineering”*, pages 117–129, Aachen, 1999. Shaker-Verlag.
- [35] A. Mielke and F. Theil. On rate-independent hysteresis models. *Nonl. Diff. Eqns. Appl. (NoDEA)*, 11:151–189, 2004. (Accepted July 2001).
- [36] A. Mielke, F. Theil, and V. I. Levitas. A variational formulation of rate-independent phase transformations using an extremum principle. *Arch. Rational Mech. Anal.*, 162:137–177, 2002.
- [37] M. Negri and C. Ortner. Quasi-static crack propagation by Griffith’s criterion. *Math. Models Methods Appl. Sci.*, 18(11):1895–1925, 2008.
- [38] C. Panagiotopoulos. Open BEM Project. <http://www.openbemproject.org/>, 2010.
- [39] F. París and J. Cañas. *Boundary Element Method, Fundamentals and Applications*. Oxford University Press, Oxford, 1997.
- [40] P. Podio-Guidugli and G. Vergara Caffarelli. Surface interaction potentials in elasticity. *Arch. Rat. Mech. Anal.*, 109:343–381, 1990.
- [41] N. Point. Unilateral contact with adherence. *Math. Methods Appl. Sci.*, 10:367–381, 1988.
- [42] N. Point and E. Sacco. A delamination model for laminated composites. *Math. Methods Appl. Sci.*, 33:483–509, 1996.
- [43] N. Point and E. Sacco. Mathematical properties of a delamination model. *Math. Comput. Modelling*, 28:359–371, 1998.
- [44] R. Rossi and T. Roubíček. Adhesive contact delaminating at mixed mode, its thermodynamics and analysis. Preprints: No.26/2011 at Univ. Brescia, and on arxiv:1110.2794. *Interfaces and Free Boundaries*. submitted.
- [45] T. Roubíček, M. Kružík, and J. Zeman. Delamination and adhesive contact models and their mathematical analysis and numerical treatment. In *Math. Methods & Models in Composites*, chapter 13. (V. Mantič, ed.) Imperial College Press, ISBN: 978-1-84816-784-1, to appear in 2012.
- [46] T. Roubíček, L. Scardia, and C. Zanini. Quasistatic delamination problem. *Cont. Mech. Thermodynam.*, 21:223–235, 2009.
- [47] J. Simo and T. Hughes. *Computational Inelasticity*. Springer, New York, 1998.
- [48] J. Swadener, K. Liechti, and A. deLozanne. The intrinsic toughness and adhesion mechanism of a glass/epoxy interface. *J. Mech. Phys. Solids*, 47:223/258, 1999.
- [49] L. Távara, V. Mantič, E. Graciani, J. Cañas, and F. París. Analysis of a crack in a thin adhesive layer between orthotropic materials: An application to composite interlaminar fracture toughness test. *CMES - Computer Modeling in Engineering and Sciences*, 58:247–270, 2010.
- [50] L. Távara, V. Mantič, E. Graciani, and F. París. BEM analysis of crack onset and propagation along fiber-matrix interface under transverse tension using a linear elastic-brittle interface model. *Engineering Analysis with Boundary Elements*, 35:207–222, 2011.
- [51] M. Thomas. *Rate-independent damage processes in nonlinearly elastic materials*. PhD thesis, Institut für Mathematik, Humboldt-Universität zu Berlin, 2010.
- [52] M. Thomas. Quasistatic damage evolution with spatial bv-regularization. (submitted), Preprint No. 1638, WIAS, Berlin, 2011.
- [53] M. Thomas and A. Mielke. Damage of nonlinearly elastic materials at small strain – Existence and regularity results –. *Z. angew. Math. Mech. (ZAMM)*, 90(2):88–112, 2010.
- [54] R. Toader and C. Zanini. An artificial viscosity approach to quasistatic crack growth. *Boll. Unione Matem. Ital.*, 2(1):1–36, 2009.
- [55] R. Toupin. Elastic materials with couple stresses. *Arch. Rat. Mech. Anal.*, 11:385–414, 1962.
- [56] V. Tvergaard and J. Hutchinson. The influence of plasticity on mixed mode interface toughness. *J. Mech. Phys. Solids*, 41:1119–1135, 1993.